ACS APPLIED MATERIALS & INTERFACES

Research Article

www.acsami.org

Barnacle Larvae Exploring Surfaces with Variable Hydrophilicity: Influence of Morphology and Adhesion of "Footprint" Proteins by AFM

Shifeng Guo,[†] Sreenivasa Reddy Puniredd,[†] Dominik Jańczewski,*[,†] Serina Siew Chen Lee,[‡] Serena Lay Ming Teo,[‡] Tao He,[†] Xiaoying Zhu,[†] and G. Julius Vancso*[,§,⊥]

[†]Institute of Materials Research and Engineering, A*STAR (Agency for Science, Technology and Research), 3 Research Link, Singapore 117602

[‡]Tropical Marine Science Institute, National University of Singapore, 18 Kent Ridge Road, Singapore 119227

[§]Institute of Chemical and Engineering Sciences, A*STAR, 1 Pesek Road, Jurong Island, Singapore 627833

[⊥]MESA+ Institute for Nanotechnology, Materials Science and Technology of Polymers, University of Twente, 7500 AE Enschede, The Netherlands

Supporting Information

ABSTRACT: Interaction forces of adhesive proteins employed by cyprid larvae of *Amphibalanus amphitrite* for temporary attachment during surface exploration in marine fouling were studied by AFM force spectroscopy using chemically modified, reactive colloidal probes. The proteins were covalently attached to the surfaces of the probes by incubation in the protein deposits (footprints) left behind at the surface by the cyprids. This covalent coupling enabled robust and reproducible probing of adhesion of the attachment proteins to model surfaces with variable hydrophilicity. Three model monolayer surfaces were designed and prepared that exhibited different wettabilities derived from variations in the monolayer chemical composition. The morphology and size of cyprid protein deposits was imaged by AFM. The deposits showed larger area of spreading on more hydrophobic surfaces, whereas the overall volume of the secreted proteins exhibited no significant variation. Notable difference in adhesion forces was found among the surfaces by force spectroscopy, with substantially higher values measured on the hydrophobic surface (21 ± 2 nN) than that measured on the more hydrophilic surface (7.2 ± 1 nN). The same surfaces were also tested in laboratory essays. Rather surprisingly, no significant differences were found in values of fractional cyprid settlement among the surfaces studied, indicating that variations of surface wettability and adhesion strength of settlement proteins may be insufficient to explain settlement trends.

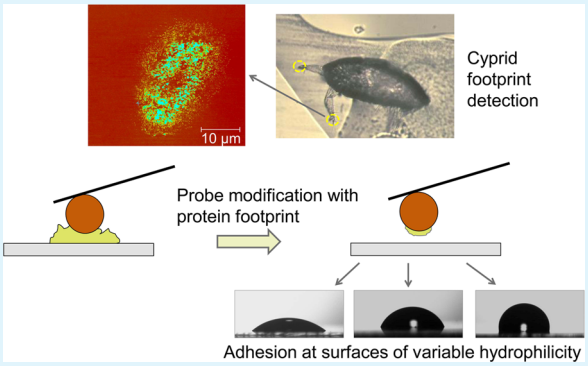

KEYWORDS: *AFM force spectroscopy, wettability, cyprid temporary bioadhesion proteins, colloidal probe, adhesion forces*

1. INTRODUCTION

Marine biofouling refers to the undesirable accumulation of marine organisms on surfaces submerged in seawater environments. This process seriously impacts marine industries, with profound economic and environmental consequences.[1] Barnacles are considered as one of the most problematic hard macrofoulers because of their size, gregarious nature, and ability to colonize nearly any man-made structure.[2]

The lifecycle of the barnacle, *Amphibalanus amphitrite* (Darwin, 1854), includes six planktonic naupliar stages, a nonfeeding cyprid larval stage, and a sessile adult stage. The cyprid, the penultimate stage of barnacle, explores the location for settlement, assesses suitability of site for the adult development and following attachment metamorphoses into the adult animal.[3] Surface exploration is performed using the adhesive discs on the paired antennules, in a form of reversible bipedal "walking", probing the substrate for surface texture, material properties, chemical clues, and presence of adult or cyprid nonspecific proteins.[4] During surface exploration, temporary adhesive proteins are deposited as "footprints" through the antennular attachment discs. These proteins form temporary anchoring points for the migrating cyprids,[5,6] and have been implicated to act as settlement cues for other exploring cyprids. The exact physiochemical nature of the temporary adhesive proteins remains largely unknown. However, a settlement-inducing protein complex (SIPC), which also functions as a settlement cue, has been found.[7−9] Therefore, in

Received: May 21, 2014
Accepted: July 23, 2014
Published: July 23, 2014

addition to serving as a putative temporary adhesive, the secretion also acts as a conspecific pheromone for other cyprids.

One of the approaches toward reducing the fouling impact of barnacles is to discourage cyprids from settlement during the exploratory stage. This may be achieved by the fine-tuning of temporary adhesive/surface interactions through tailoring the chemical and physicochemical surface properties.[10] To design effective antifouling surfaces, we require a better understanding of the interactions between the temporary adhesive proteins and different surfaces.

Deposits of cyprid temporary adhesives proteins were visualized by scanning electron microscopy imaging.[11] As these images were captured under dry conditions, these observations likely have not been characteristic for the hydrated condition of the adhesive material deposited. Indirect footprint observations have been described using staining the areas explored by cyprids by coomassie blue Bio-Rad protein dye reagent (CBB) or anti-76 kDa antiserum. The measured footprint sizes were in good agreement with the antennular disc diameters of cyprids.[7,12] The proteinaceous footprints can also be visualized using surface plasmon resonance imaging.[13] Although the discovery of the adhesive secretion and "footprint" deposition was a significant step toward a better understanding of barnacle attachment, corresponding studies have not provided information on the fine structures of the footprint proteins and have not included examination of the adhesive behavior associated with reversible cyprids attachment. The use of atomic force microscopy (AFM) enabled the morphology of the deposited temporary adhesives of cyprids to be clearly visualized.[14,15]

Previous studies suggest that colonization of the substrate by cyprids is affected by the adhesion between the temporary adhesive and substrate surface. Measurements of the temporary adhesives strength of cyprids larvae of *Balanus balanoide* were conducted first using a sensitive balance.[5] The live cyprid was attached to a thin metal wire using a cyanoacrylate adhesive, and once the animal started walking on the submerged surface, the surface was gently lowered and the detachment force was measured. However, this study was empirical and did not involve the direct measurement of adhesion between the protein deposits and the substrate surfaces. Thus, the adhesive process was not directly reflected by the data.[16] Interaction forces of proteinaceous footprint proteins (FP) have been also studied using AFM.[14] In this work, the interaction force between the AFM tip and the FP materials was measured and the adhesion forces were estimated by scaling up the interaction forces of FP materials and AFM tip to the size of footprints. As a model investigation, Schön et al.[17] reported AFM-based force spectroscopy studies using colloidal probes functionalized with adhesion proteins (fibronectin). In this study, the authors explored adhesion forces at nonfouling and fouling protein brush surfaces and demonstrated substantial suppression of protein adsorption on zwitterionic sulfobetain brushes by AFM force spectroscopy. The AFM force spectroscopy has been also used to study the adhesion properties of mussel bioadhesive using DOPA functionalized AFM tip.[18]

Protein−surface interactions are affected by the protein's properties as well as by the properties of the surfaces, including surface energy, polarity, charge and morphology.[19,20] Surface affinity to water defined by its hydrophobic or hydrophilic character and generally referred as wettability, is an important parameter affecting the biological response of exposing the materials to the environment. The effect of surface wettability on protein adhesion has been extensively studied.[21−24] Surface wettability has also been reported as an important parameter affecting the attachment of barnacle cyprids and the widely held view has been that cyprids have a preference for "high-energy"/hydrophilic surfaces.[25−29] However, different opinions have also been presented, highlighting that surface chemistry and specifically charge, rather than the surface wettability, is responsible for the choice of cyprid settlement.[30−32] Separating the influence of surface charge from other interactions that cause a variation in wettability is particularly important since in previous studies various surface parameters e.g. wettability and surface charge were not sufficiently decoupled from each other. Hence conclusions about the individual contributions of the various interactions to adhesion forces could not have been obtained.

In this work, we evaluated a series of model surfaces and their interactions with cyprid temporary adhesive proteins using AFM experiments. A series of custom-made monolayers with different affinity to water were designed and synthesized with the specific aim to avoid Coulombic charge interactions. These model surfaces were used to study the influence of surface wettability on the secretion of barnacle proteins. The interaction of cyprid footprint proteins with surfaces were evaluated using colloidal probe based AFM force spectroscopy. Footprint proteins were covalently attached by chemical coupling to previously chemically activated colloidal AFM probe. This allowed us to perform direct measurements of adhesion forces between substrate and proteins to provide new insights into adhesion in the seawater environment.

2. MATERIAL AND METHODS

2.1. Materials. Tromethamine, dimethylaminopyridine (DMAP), and N-diisopropylethylamine (DIPEA) were purchased from Sigma-Aldrich. Dimethyl sulfoxide (DMSO), acetone, and isopropanol were supplied by Tedia and were used directly without further purification; 11-Pentafluorophenylundecanoatetrimethoxysilane was bought from Sikemia. Silicon wafers (Latech Scientific Supply Pte. Ltd.) and glass coverslips (Deckglaser, Germany) were used for surface preparation of the substrates. Deionized (DI) water with resistivity of 18 MΩ cm^{-1} was obtained from a Millipore Nanopure system.

Silicon wafers (2 cm × 2 cm) and glass coverslips were cleaned using acetone and isopropanol in ultra sonicator for 10 min each, followed by rinsing with deionized (DI) water and nitrogen gas drying. Subsequently, the surfaces were treated with oxygen plasma (Duratek, Taiwan) at 200 W for 5 min to create a surface rich in hydroxyl groups at the oxide surface to facilitate the subsequent silanization process. Hydroxyl-covered glass and silicon substrates were placed in a desiccator and exposed to 11-pentafluorophenylundecanoatetrimethoxysilane under vacuum at 150 °C for 3 h. The surfaces terminated with pentafluoro activated ester were named as PFP terminated monolayers.

The PFP-terminated surfaces were exposed to a solution of 250 mM tromethamine in dry dimethyl sulfoxide (DMSO) for 48 and 72 h at 60 °C in the presence of DMAP and DIPEA. The samples were rinsed and sonicated subsequently in DMSO and acetone prior to the surface analysis. See Figure 1 for illustration of the preparation process.

2.2. Surface Characterization. Static water contact angle measurements were carried out using a KSV CAM 200 goniometer (KSV Instruments). Drops of 5 μL of DI water were automatically dispensed at the surface of the specimens, and the water contact angles were determined with a CCD camera using a tangential method. For each measurement, five readings were taken using different spots and an average was calculated.

X-ray photoelectron spectroscopy (XPS) scans were obtained from a VG ESCALAB 250i-XL spectrometer using an Al Kα X-ray source (1486.6 eV photons). The core-level signals were obtained at a photoelectron take off angle of 90° (with respect to the sample surface). The X-ray source was run at a reduced power of 150 W. The pressure in

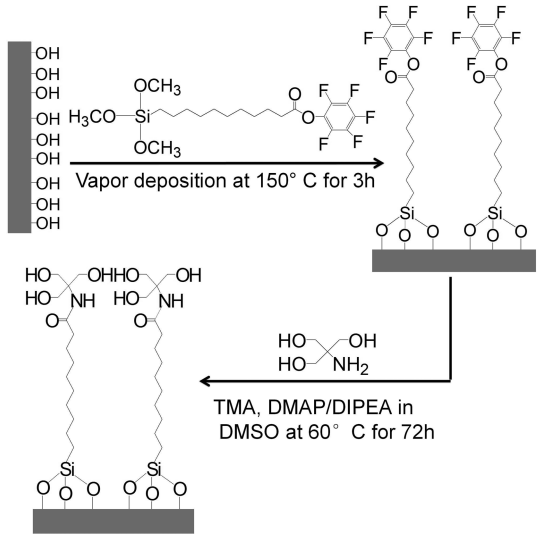

Figure 1. Schematic of substrate surface preparation.

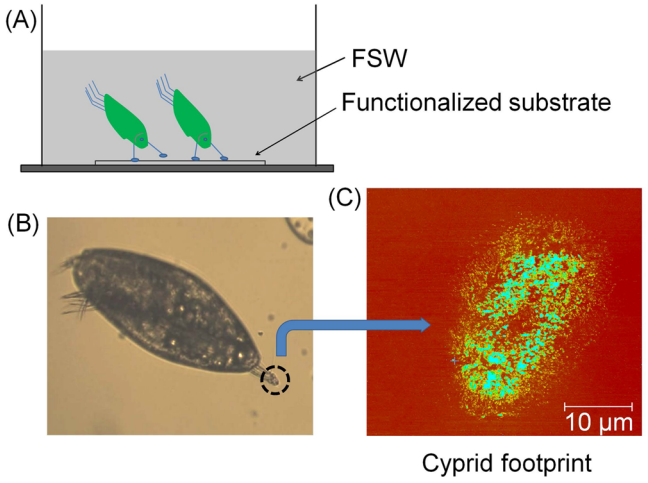

Figure 2. Process of cyprid FPs detection. (A) Cyprids were introduced at model surfaces in FSW; (B) cyprid walking behavior was observed and the explored area was marked; (C) cyprid footprint was scanned in FSW condition using AFM.

the analysis chamber was maintained at 1×10^{-6} Pa or lower during each measurement. Binding energies were calibrated with carbon (C 1s, 285 eV). Survey spectra were run in the binding-energy range of 0−1000 eV, and the high-resolution spectra of C 1s, N 1s, and F 1s were collected.

The surface morphology of the model surfaces was visualized by tapping mode AFM imaging under ambient conditions using standard silicon probes ($k \approx 40$ N/m, Tap 300AL-G, Budget sensors).

2.3. Cyprid Culture. Barnacle cyprids were reared at the Marine Laboratory of the Tropical Marine Science Institute (TMSI), National University of Singapore. Larvae spawned from the adults were collected from the Kranji mangrove area, Singapore, and were fed by an algal mixture of 1:1 (v/v) of *Tetraselmis suecica* and *Chaetoceros muelleri* at 26 °C, at a density of 5×10^5 cells/mL approximately.[33] Barnacle larvae developed into the cyprid stage within 5−7 days. The cyprids were stored at 4 °C and used for AFM experiments within 5 days. Cyprids were acclimated to room temperature for 10 min before experiments were initiated.

2.4. Characterization of FP Proteins by AFM. A Nanowizard III instrument (JPK Instruments AG, Berlin, Germany) equipped with the NanoWizard head and controller was used in all AFM experiments. To remove any possible contamination, we first cleaned the AFM tips using freshly prepared piranha solutions (mixture of 70% H_2O_2 and 30% H_2SO_4) for 5 min, followed by oxygen plasma (Duratek, Taiwan) treatment at 100 W for 90 s. The morphology of cyprid temporary adhesive proteins (FPs) was imaged using triangularly shaped silicon nitride cantilevers (Nano World, PNP-TR) in autoclaved filtered seawater (FSW, filtered 0.2 μm) condition. The spring constant of the cantilevers was calibrated using the thermal noise method,[34] and values found were in the range of 0.07−0.09 N/m. The quantitative imaging (QI) mode, which is a force spectroscopy based imaging mode used by JPK Instruments, was used to image the FPs. To evaluate the effect of surface wettability on the secretion of cyprid FPs, 12 FPs for each surface were imaged. Every FP was obtained from a different individual animal.

The location of multiple FPs in situ was found through optical observation of the cyprid exploration prior to the AFM measurements. The method is schematically shown in Figure 2. The investigated glass coverslip substrate (1 cm × 1 cm) was first glued on a larger glass slide (25 cm × 76 cm), sealed with the AFM liquid cell and fixed on the AFM stage. Cyprids were first introduced into a polystyrene Petri dish, and the behavior of cyprids was observed. Once an active cyprid was detected, it was collected and transferred carefully onto the sample surface (chemically modified glass coverslip) using a micropipette. The cyprid behavior was observed by the video capture software which is incorporated in the JPK AFM system. When the cyprid started to explore the surface, the areas with the FPs deposits were marked on the image. (A typical video depicting this process is available as Supporting Information.) The surface explored was gently washed using FSW, and the AFM liquid cell was filled with fresh FSW. Finally, the AFM scan head was assembled and the cantilever was positioned to the areas where FPs were previously found and marked.

In force spectroscopy experiments, colloidal contact probes with SiO_2 sphere (with a diameter of 5 μm) (NT-MDT, Russia) were used. Prior to modification, the probe was first incubated in ethanol for 1 h followed by rinsing with Millipore water and drying with N_2 gas. Subsequently the probe was treated using oxygen plasma (Duratek, Taiwan) at 120 W for 90 s to remove possible organic contamination and to create a surface rich in hydroxyl groups. The pretreated probe was amino-functionalized with aminopropyl trimethoxysilane (APTMS) using vapor deposition as described previously.[35,36]

The NH_2-terminated probe was immersed in an aqueous solution of 2.5% glutaraldehyde and reacted with it. The thus formed layer was used as the binding agent to attach the proteins of interest to the colloidal probe.[37−40] The probe was then gently rinsed using Millipore water after 2 h immersion (Figure 3). The colloidal probe was immersed in FPs consisting of cyprid temporary adhesive proteins, detected as described

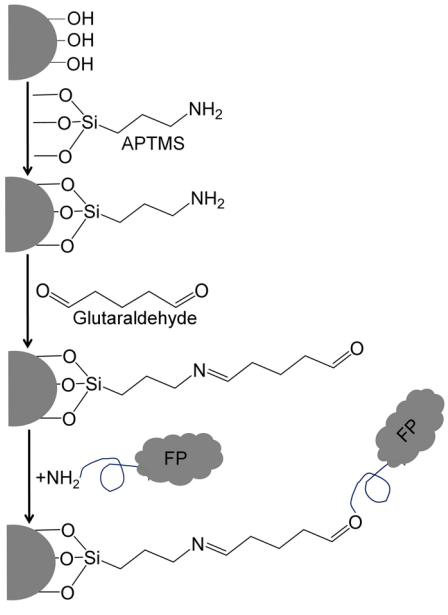

Figure 3. Chemical modification process of the colloidal probe using cyprid temporary adhesive proteins.

dx.doi.org/10.1021/am503147m | ACS Appl. Mater. Interfaces 2014, 6, 13667−13676

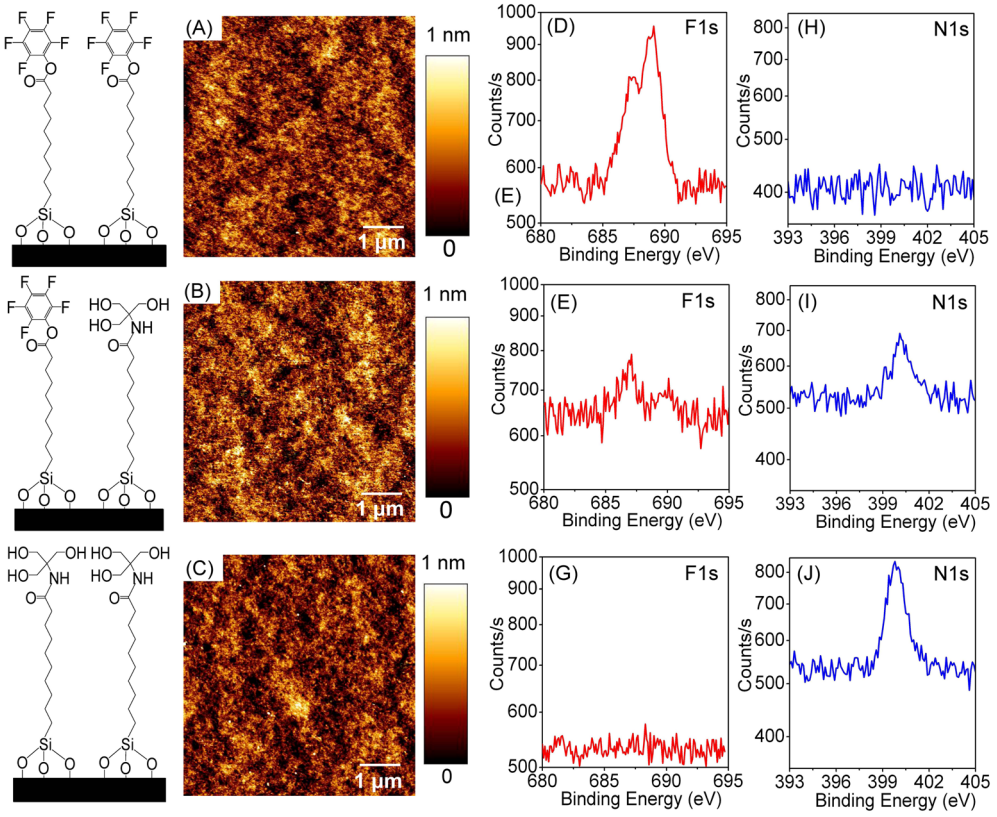

Figure 4. AFM topography and XPS F 1s and N 1s spectra for the high (panels A, D, and H), medium (panels B, E, and I) and low (C, G, and J), contact angle surfaces, respectively. Counts/s represents counts/second.

in section 2.4, for 3 h and subsequently rinsed gently using FSW to remove the physical adsorbed material. Cyprid FP modified probes (FPCP) were used immediately following probe functionalization for the adhesion experiments. Before and after the experiments the spring constant of the cantilevers were calibrated using the thermal noise method (0.07−0.1 N/m). All force curve measurements between FPCP and surfaces were performed in FSW, using a fluid cell and allowing the system to equilibrate for 30−60 min.

2.5. Settlement Assay. Cyprid settlement assays were conducted to evaluate the effect of surface wettability on the preferences of cyprid attachment. Nine replicates of every substrate surface were evaluated. The "droplet" assay was carried out with 300 μL of seawater containing approximately 20−30 cyprids used for each surface.[41] The substrates were kept inside a 35 mm Petri dish with lid on to minimize evaporation of FSW droplet in a humidity chamber. The assay was incubated at 26−28 °C for 24 h, on a 12 h light and 12 h dark period. The cyprids were then examined under a stereo microscope (Nikon SMZ 1500, Japan), and all settled cyprids were counted, including those that were permanently attached, but not metamorphosed. Fouling performance is calculated as the fraction of settled cyprids against all animals in the experiment.

2.6. Statistical Analysis. Statistical comparisons were performed using GraphPad Prism 5 (GraphPad Software Inc.). Data of surface wettability on the cyprid FP sizes, adhesive forces and settlement were analyzed with a one-way analysis of variance (one-way ANOVA), followed by a Tukey post-test. All data were reported as mean ± standard error (SE). For all comparisons, $p \leq 0.05$ were considered as statistically significant.

3. RESULTS AND DISCUSSION

3.1. Preparation and Characterization of Substrates. Earlier studies probing the influence of surface wettability in protein adhesion and biofilm formation have employed short or long chain self-assembled monolayers with specific, well-defined functional groups.[22,31,42] In this work, we used three different molecular monolayers which display an increasing affinity to water across the series. This was achieved by deposition of 11-Pentafluorophenylundecanoate- trimethoxysilane (PFP) as the base monolayer followed by subsequent chemical modification by the reaction of ester with tromethamine (Figure 1). Chemical groups with permanent ions in water were intentionally excluded for this design. As a consequence, the series of monolayers provided surfaces characterized by minimal Coulombic charge component (ion−ion interactions) and allowed us to investigate adhesion forces predominantly derived from hydrophobic interactions of footprint proteins with substrates.

3.2. Characterization of the Model Surfaces. Static water contact angle values of silicon/glass surfaces after oxygen plasma cleaning were <10°, which indicated a very hydrophilic surface. PFP modified surfaces showed contact angles in the range of 90−95°; these values are consistent with the literature.[43] The presence of the alcohol groups were clearly shown by significant changes in the wettability of the substrates. The contact angle of the PFP monolayer decreased from 90−95° to 65−70° and 40−45° after immersion in tromethamine solutions for 48 and 72 h, respectively. The wettability results indicate successful reaction between the amine groups of tromethamine and activated ester of pentafluorophenyl ester silane at the surfaces. Developed materials with contact angles of 90−95°, 65−70°, and 40−45° are referred to as high (95°), medium (65°), and low (40°) contact angle surfaces, respectively. The schematic illustration of the primary and secondary modification of silicon/glass surfaces is shown in Figure 1.

In addition to contact angle measurements, XPS was used to characterize the high, medium and low contact angle surfaces. Presence of F 1s and absence of N 1s peaks after the surface

modification with PFP silane were indicative of the successful monolayer attachment to the surface (Figure 4D, H). The F 1s XPS spectrum decreased for the medium contact angle surface (Figure 4E), and disappeared entirely for the low contact angle surfaces (Figure 4G). The evolution of N 1s spectrum (Figure 4I) upon reaction with tromethamine proved the successful formation amide bonds. The stronger N 1s peak and the absence of F 1s peak showed that there was quantitative conversion of fluorinated activated ester to alcohol terminated surfaces through amide bonding (Figure 4G, J). The atomic composition for all elements is presented in the Supporting Information (Table S1).

The model surfaces were visualized in air using tapping mode AFM. The morphologies are shown in Figure 4A–C. The monolayer modified surfaces were flat with the similar average roughness (R_q) values around 200 pm (Table 1). Therefore, the

Table 1. Characterization of Different Wettability Surfaces

chemically modified surfaces	low	medium	high
static water contact angles (deg)	40–45	65–70	90–95
roughness (R_q) (pm)	190 ± 27	200 ± 19	185 ± 22

effect of surface roughness on cyprid FPs secretion across the different treatments may be assumed to be the same. All AFM measurements were collected using a scan area of 5 μm × 5 μm.

3.3. Comparison of FP Morphology at Surfaces with Different Wettability. Visualization of the morphology of FPs by AFM provides clues to better understand interactions of adhesion proteins with the confining materials at their interfaces with the substrate and seawater, as well as molecular organization within the proteinaceous layer. Morphology maps of the cyprid FPs at the modified glass surfaces were obtained in FSW (0.2 μm autoclaved filtered seawater) immediately following removal of the cyprids after exploration steps. Imaging of the entire footprints in FSW provides a fairly realistic picture of the actual morphology and FP size. All FPs observed in this study were elliptical in shape, with diameters of approximately 20–40 μm. The morphologies observed in this study confirm earlier observations,[44] which displayed a microfibrillar protein structure with fibers of varying diameter, deposited in a somewhat ordered fashion following the circumference of the footprint ellipse. The central region of the ellipse showed a depletion in proteins (Figure 5A-C), which can be related to the contact process between the cyprid antennules and substrate during withdrawal of the organ at the end of the protein secretion. The heights of nanofibrils of FPs as estimated by AFM height section (Figure 5E–G) varied between 10 and 100 nm, indicating the presence of bundles of proteins aggregates that were secreted during surface exploration. The height of FPs on the high contact angle surfaces was found larger that on the medium and low contact angle surfaces.

The morphologies of FPs deposited at substrate surfaces with different wettabilities appeared to have different dimensions, with the largest spread on the hydrophobic surfaces as compared with the medium and hydrophilic surfaces (Figure 5A-C). However, the thickness of FPs on the high contact angle surface was smaller, which was reflected from the cross section of the FPs. The geometrical information on FPs at surfaces with different wettability is displayed in Figure 6. The average value of the FP area on the low contact angle surface was 287 ± 60 μm^2. This is much smaller than the values observed at surfaces with high contact angles, which were 465 ± 90 μm^2 (Figure 6). This observation is consistent with previous findings[14,44] that the

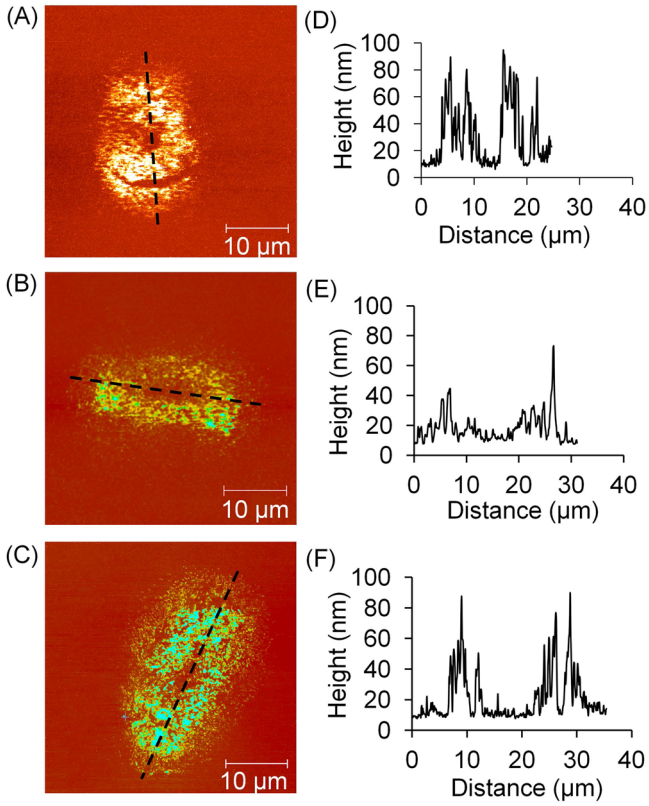

Figure 5. Representative AFM images of cyprid FPs deposited on different wettability surfaces. (A) The FPs on the low contact angle surface; (B, C) FPs on the medium and high contact angle surfaces; (D–F) cross-sectional plot of FP from height along the dashed line for surfaces A–C, respectively.

temporary adhesive proteins, both from *B. improvisus* and *B. amphitrite* cyrids, spread over a larger area on the hydrophobic surfaces (CH_3-terminated). The FPs deposited on the lowest contact angle surfaces consisted of thick protein aggregates, with a height of 22 ± 5 nm, which is approximately two times thicker than the values found for FPs deposited on the medium and high contact angle surfaces. The overall volume of FPs, representing the total amount of proteins deposited is similar and is in the range of 4.7–6.5 μm^3 for all substrate surfaces imaged. The volume of FPs in the native hydrated condition was found to be twice as large as that obtained during imaging in dry condition.[44]

The largest deposit area observed for hydrophobic model monolayer surface indicates that footprint proteins are predominantly hydrophobic or experience conformational changes leading to exposure of hydrophobic domains when in contact with hydrophobic surface. Studies have shown that many proteins undergo conformational changes during the adsorption to a solid surface and tend to maximize their area of contact by conformational reorganization.[20,45] Surface wettability is an important parameter that affects protein adsorption, and proteins tend to adsorb on the hydrophobic surface by hydrophobic patches of residues present in the structures.[46] Generally proteins adhere stronger to hydrophobic surfaces with the adsorbed proteins tend to occupy a greater area of the substrate surface.[21,24]

3.4. Adhesion between Footprint Proteins and Surfaces of Variable Hydrophilicity. To measure interaction forces between the cyprid temporary adhesive proteins and the surfaces with different wettability prepared in this study, we

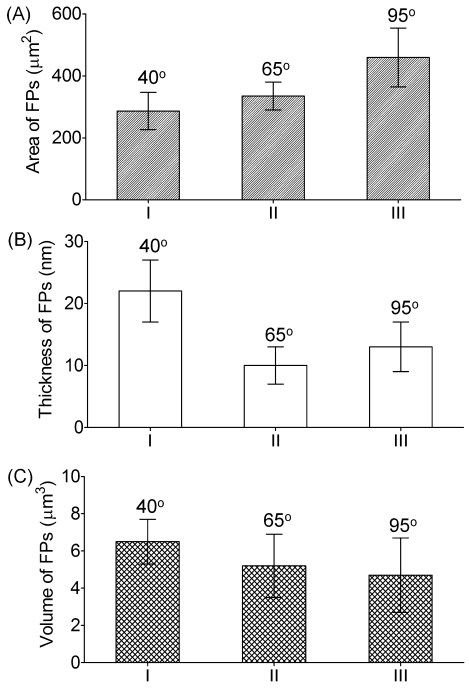

Figure 6. Geometric data of FPs at substrate surfaces with different wettability values. Water contact angle value for each surface is provided above the bars. The low, medium, and high contact angle surface is represented by the symbols I, II, III, respectively. (A) Average FP area vs contact angle; (B) average FP thickness vs contact angle; (C) average FP volume vs contact angle. Error bars correspond to standard errors. The area and thickness values of cyprid FPs are significantly affected by surface wettability (one-way ANOVA, $p \leq 0.0001$). The FP areas on the high contact angle surfaces (95°) are significantly larger than the values on the low contact angle surfaces (40°) (Tukey test, $p \leq 0.05$), whereas the largest FP thickness is found on the low contact angle surface (40°) (Tukey test, $p \leq 0.05$). No significant difference in FP areas and thickness is found between medium (65°) and high contact angle surfaces (Tukey test, $p > 0.05$). Also, there is no significant difference in the FP volumes among the surfaces (Tukey test, $p > 0.05$).

performed AFM-based force spectroscopy experiments using colloidal probes functionalized with FP proteins (FPCP). The schematic of the experimental process is shown in Figure 7. The colloidal probe (Figure 7A) was first chemically treated, as described in detail in the experimental section, and subsequently modified by incubation in the footprint deposits to covalently attach proteins to the probe (Figure 7B). The aldehyde groups of glutaraldehyde at the colloid surfaces form imine links between primary amine groups of the protein and those at the tip surface,[36,40,47] which ensures covalent attachment.

The force curve measurements were conducted at a vertical scan rate of 0.5 Hz with a z ramp size of 1 μm; the "set point" of the loading force was kept the same at 2.9 nN for the three surfaces. Force data were collected using the force mapping imaging mode (as defined by JPK) resulting in a 14 × 14 array of force curves over a scan area of 10 μm × 10 μm, with 196 force curves acquired. Three different areas selected resulting in a total number of 500 curves analyzed for each surface with specific wettability (see the Supporting Information)

During the experiments, the FPCP is repeatedly approached and retracted by a piezo scanner as it moves across the different areas of the investigated substrates (Figure 7C). No protein transfer occurred during the measurement from the probe to the substrate, which was verified by the consistent force curves obtained on each surface (for a representative collection of force curves, see the Supporting Information). Thus, the glutaraldehyde linkages provide strong binding between proteins and probe, ensuring no protein desorption from the probe during force measurements.

The force curve capturing process of FPCP with a surface is shown in Figure 7D and typical force distance curves (approach and retraction) between FPCP and the surfaces are shown in Figure 7E–G. When the probe is being separated from the surface, the usually weaker noncovalent bonds between the protein and the surface are compromised. The bonds are terminated as sacrificial bonds as introduced by Hansma et al., which include hydrogen bonds, hydrophobic and electrostatic protein interactions.[48] The combination of chemical and mechanical factors leads to the observed "pull-off" or adhesion force when the probe withdraws from the surface. When the piezo scanner was retracted from the substrate, the probe continued to stretch and detach more sacrificial bonds.[49,50] Sawtooth shaped retraction force curves were observed (Figure 7E–G), suggesting multiple interactions within protein secondary structure and between protein and the substrates during tip separation from the surfaces, as a result of the sacrificial bond rupturing.

During retraction, the force curves exhibit an overall maximum, which we defined as adhesion force. Because energy dissipation related to changes of protein molecular conformation, viscoelastic effects and other processed is also taking place during the experiment, the retraction events provide information about the combination of adhesion and adherence (adherence referring to dissipative processes). For simplicity, and in line with most literature references, we use the terminology "adhesion" for the combined effects observed.

The probing process is shown in Figure 7E–G. Values of the maximum magnitude of pull-off forces were used to obtain force histograms for the different substrates. The distributions are shown in Figure 8A–C, and the values of the average adhesion forces are summarized in Figure 8D. From these data we conclude that the adhesion force of FPs has a very sensitive response to the surface wettability. The adhesion forces show a clear shift toward larger values when the experiments were conducted on the more hydrophobic surfaces.

On the low contact angle surface (40°), smaller average rupture forces with values around 7.2 ± 1 nN were recorded. Higher values were observed on the larger contact angle surfaces. The forces obtained from the medium contact angles surface (65°) were 11 ± 1.3 nN. The values of the highest forces on the hydrophobic surfaces (95°) exhibited values in the excess of 20 nN. A similar trend was observed for the adhesion energy, which was computed as the area under the force–distance retraction curve with the baseline taken at zero force to subtract the area under the force–distance approaching section[51] (see the Supporting Information, Figure S1). The adhesion energy on the low, medium, and high contact angle surfaces are 1.2 ± 0.4, 1.5 ± 0.4, and 3.9 ± 0.6 × 10^{-15} J, respectively. More energy was required to retract the FPs material from the hydrophobic surfaces. However, no significant difference was observed between low and medium contact angle surfaces.

Protein adhesion is affected by a combined effect of van der Waals, hydrophobic, ionic interactions and hydrogen bonding.[20] Although surface–protein interactions are complex in nature, the properties of surfaces have been reported to play a fundamental role in protein adhesion.[19,46] Surface wettability is a vital parameter that affects the adhesive strength of proteins.[24,52]

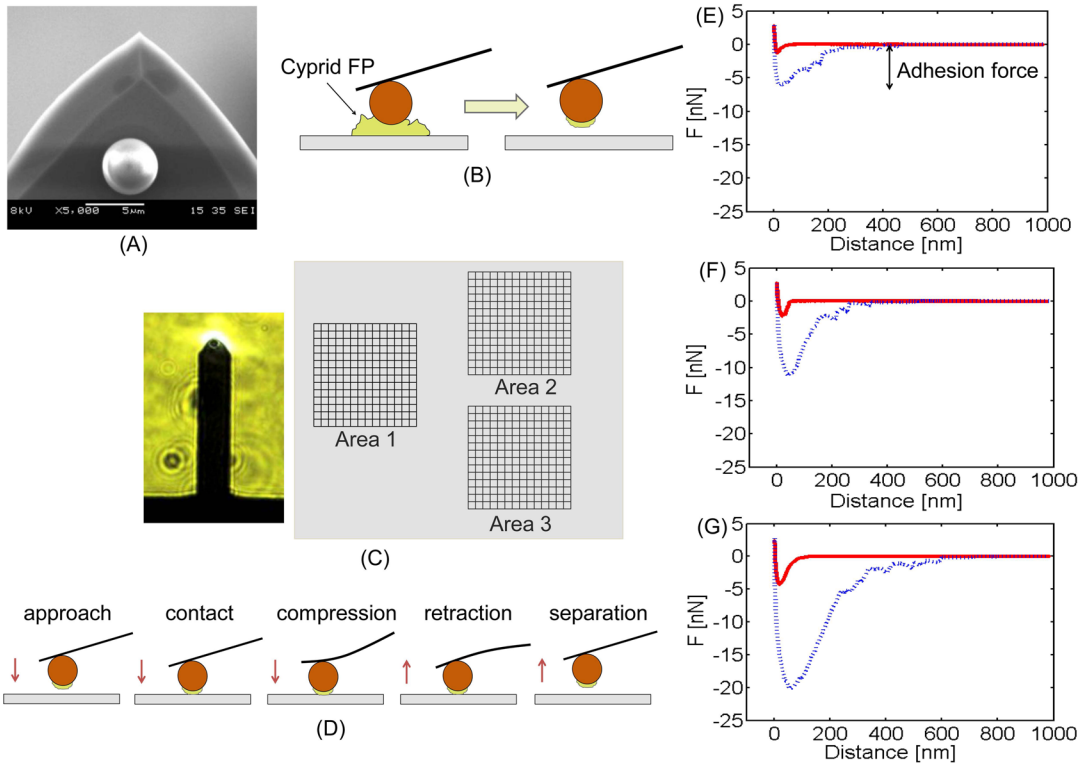

Figure 7. Schematic of the force spectroscopy experiment. (A) SEM image of colloidal probe. (B) Probe modified with FP proteins. (C) Force measurements were conducted using the force imaging mode (as defined by JPK), resulting in a 14 × 14 array of force curves over a scan area of 10 μm × 10 μm. Three different areas were selected on each surface with a chosen wettability. (D) Probe−substrate interaction during force curve measurements. (E) Representative force curve of FPs with low contact angle surface (40°). The red continuous curves represent the approach and the blue dashed line is the retraction curve. The maximum force magnitude during withdrawal with respect to the zero force baseline is defined as the adhesion force. (F) Force−distance curve of FPs with medium contact angle surface (65°) and (G) with high contact angle surface (95°).

Although observations regarding the effects of surface wettability on protein adhesion have not always been consistent, in general, higher adhesion forces were observed on hydrophobic surfaces due to strong hydrophobic forces. Increased adhesion strength on the low wettability surfaces was reported by observing seven proteins tested in an earlier study.[45] The effect of surface wettability on the adhesion of the mussel proteins has also been reported,[53] and the mussel foot proteins were found to have a unique array of hydrophobic amino acid residues that contribute to the hydrophobic adhesion to hydrophobic surfaces.

The interaction of hydrophobic (−CH_3 terminated) as well as hydrophilic tips (−OH terminated) with the FP materials was studied and strong forces were found for hydrophobic tips.[50] This was explained by assuming that the hydrophobic tip excluded the water molecules from the contact area and changed the conformation of FP proteins, resulting in strong adhesive forces via hydrophobic−hydrophobic interactions.

Current findings also support view that FPs are predominately hydrophobic in nature. However, at this stage, we are unable to conclude if FP proteins are entirely hydrophobic as released from the cyprids gland, or achieved their hydrophobic nature through conformational changes and exposure of hydrophobic domains upon contact with surfaces.

Presented results allow us to conclude that the observed increase of adhesion strength in the substrate series covered here between hydrophilic (40°) and hydrophobic (95°) surfaces is mainly driven by hydrophobic interactions of FP proteins with substrate. Surfaces discussed in this work eliminated direct Coulombic charge to charge interactions by design. Dipol-dipol or dipol-ion interactions cannot be entirely excluded from consideration, but because observed adhesion was lower on dipol rich hydrophilic surface (40°) it can be expected that those interactions are not playing a significant role. Finally hydrogen bonds are also listed as an important factor affecting the protein adhesion strength.[48,54] This effect also seems not to be prominent for the FP proteins. For the low contact angle surface with large number of OH groups the adhesion is substantially lower than on the hydrophobic surface. Because this surface is expected to promote hydrogen bonding, it may be deduced that hydrogen bonds are not playing an essential role here and forces derived from hydrophobicity are dominant particularly for experiments carried out in seawater environment. Similar results were found on BSA proteins, which showed weaker attraction to the hydrophilic surface modified with OH groups (hydrophilic) than hydrophobic surface modified with CH_3 groups.[19,45]

To check the possible loading rate effects, we investigated the magnitude of rupture forces as a function of pulling velocity (piezo retraction rate). The loading rate effects was investigated at 0.2, 0.5, and 1 μm/s. Twenty force curves were obtained in each scan area of 10 μm × 10 μm with a fixed z ramp length. Three surface areas were selected, with a total of 60 measurements taken from different locations for each pulling velocity. The experiments were performed on the fixed delay of 0.5 s between cycles for all the pulling velocities tested. No differences in pull-off force (adhesion force) regarding the pulling velocity were observed for all the surfaces tested (see the Supporting Information, Figure S2). The results are consistent with previous finding which also reported that scan rate did not affect FP adhesion forces in the experimentally accessible loading rate range.[49] The absence of the scan rate indicates that

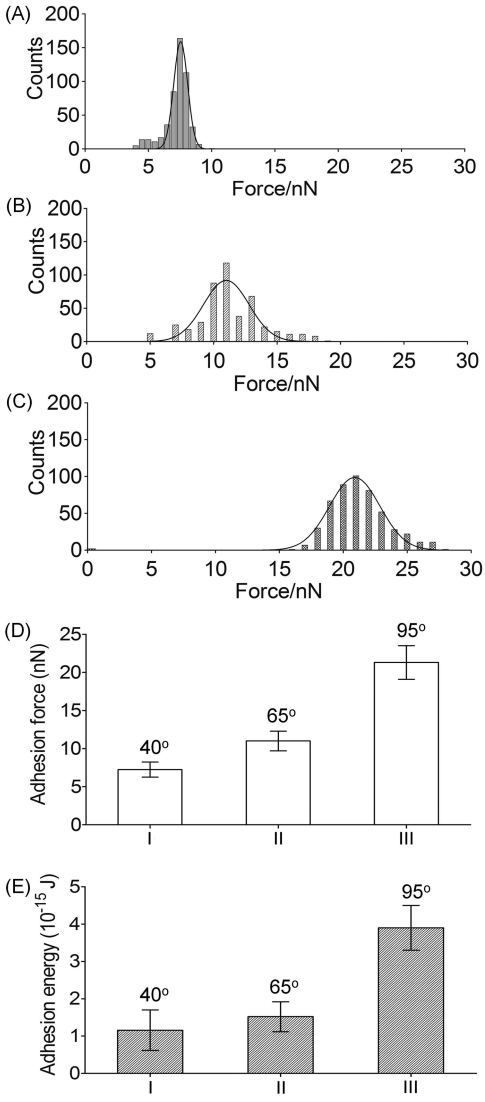

Figure 8. Distributions of pull-off adhesion forces of cyprid FP modified colloidal probes in contact with surfaces showing different wettability. (A–C) Force distributions of FP adhesive forces on low (40°), medium (65°), and high (95°) contact angle surface; (D) average adhesive forces of FPs on low, medium, and high contact angle surfaces; and (E) adhesion energy. The error bars correspond to standard errors. Surface wettability significantly affects FP adhesion force and energy (one-way ANOVA, $p \leq 0.001$). The adhesion force and energy measured on the low and medium surfaces are significantly lower than the values obtained on the high contact angle surfaces (Tukey test, $p \leq 0.05$).

unbinding of the proteins was probed in the quasi-equilibrium state.[55−57]

3.5. Cyprid Settlement Assays on the Model Surfaces with Different Wettability. Laboratory settlement tests were carried out to correlate the observed FP-surface interactions with the settlement behavior of cyprids. No significant difference in cyprid settlement was observed among the surfaces from the laboratory tests as similar fraction of organisms was colonizing all investigated substrates (Figure 9). As demonstrated in this study, surface wettability showed great impact on the morphology and adhesive strength of cyprid FP proteins. However, apparently, it did not affect cyprid settlement. Because the observable differences in adhesion of FP protein forces are significant, we may speculate that cyprids should be able to sense these

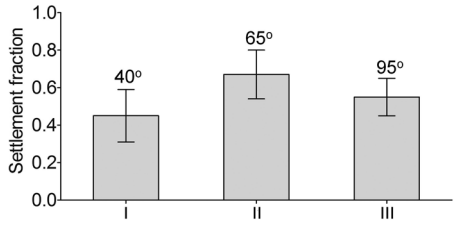

Figure 9. 24 h settlement assay of barnacle cyprid on different contact angle surfaces. The error bars correspond to standard errors. No significant difference in cyprid settlement is found among the surfaces of different wettability (one-way ANOVA, $p > 0.05$).

differences during the exploration stage. However, this has not led to a difference in the final settlement choice.

Current views about settlement behavior in relation to surface wettability and surface energy are conflicting. Some reports state that cyprids have a preference for "high-energy" surfaces.[25,28,29] However, hydrophilic zwitterionic surfaces, possessing high surface energy, inhibit cyprid settlement, suggesting that high surface energy alone is not the decisive parameter determining settlement.[58−60] There are also reports suggesting,[31,32] no correlation between surface wettability and settlement and propose that surface chemistry, or charge, rather than the surface wettability, may be responsible for choices in cyprid settlement. These observations emphasize the importance of careful design of model surfaces for settlement studies, in particular paying attention to a clear separation of contributions from different types of interactions.

4. CONCLUSIONS

Model surfaces fabricated by modification of silane monolayers were used to study the effect of surface wettability on barnacle cyprid exploratory behavior and settlement habits. Cyprid FP proteins were investigated with AFM, and different morphologies were detected on the silane monolayer modified surfaces with variable hydrophilicity and the contact angles in the range of 40−90°. Largest FP spreading areas were observed on the high contact angle surfaces, but the thickness of the FPs was the smallest among the surfaces. The adhesion forces of FPs were first evaluated using colloidal probe-based AFM force spectroscopy directly in seawater. The strongest adhesion was found on the hydrophobic surfaces as compared to the medium and hydrophilic surfaces indicating strong hydrophobic character of the FP protein. Low adhesion to hydrophilic, hydroxyl rich, surfaces suggests that hydrogen bonding is not playing an important role in FP interactions with surfaces. Although surface wettability affected the morphology and adhesion properties of FPs, it did not affect cyprid settlement behavior. Thus, for the design of antifouling materials, surface wettability alone may not be considered as the single key parameter to prevent settlement. Surface charge, which was reported to play more important role on the barnacle cyprid settlement, will be explored using the AFM-based force spectroscopy method in future.

■ ASSOCIATED CONTENT

Ⓢ Supporting Information

Collection of force curves, adhesion energy curves, scan rate effects on adhesion forces, XPS atomic composition for different wettability surfaces, and video of the optical location of cyprid footprints recorded prior to AFM measurements. This material is available free of charge via the Internet at http://pubs.acs.org/.

AUTHOR INFORMATION

Corresponding Authors

*E-mail: janczewskid@imre.a-star.edu.sg. Tel.: +65 6874 5443. Fax: +65 6872 0785.

*E-mail: g.j.vancso@utwente.nl. Tel.: +31 53 489 2974. Fax: +31 53 4893823

Notes

The authors declare no competing financial interest.

ACKNOWLEDGMENTS

The authors are grateful to the Agency for Science, Technology and Research (A*STAR) for providing financial support under the Innovative Marine Antifouling Solutions (IMAS) program.

REFERENCES

(1) Yebra, D. M.; Søren, S.; Johansen, K. D. Antifouling Technology-Past, Present and Future Steps towards Efficient and Environmentally Friendly Antifouling Coatings. *Prog. Org. Coat.* **2004**, *50*, 75−104.

(2) Crisp, D. J.; Meadows, P. S. The Chemical Basis of Gregariousness in Cirrioedes. *Proc. R. Soc. B* **1962**, *156*, 500−520.

(3) Aldred, N.; Clare, A. S. The Adhesive Strategies of Cyprids and Development of Barnacle-resistant Marine Coatings. *Biofouling* **2008**, *24*, 351−363.

(4) Schumacher, J. F.; Aldred, N.; Callow, M. E.; Finlay, J. A.; Callow, J. A.; Clare, A. S.; Brennan, A. B. Species-specific Engineered Antifouling Topographies: Correlations between the Settlement of Algal Zoospores and Barnacle Cyprids. *Biofouling* **2007**, *23*, 307−317.

(5) Yule, A. B.; Crisp, D. J. Adhesion of Cypris Larvae of the Barnacle, *Balanus Balanoides*, to Clean and Arthropodin Treated Surfaces. *J. Mar. Biol. Assoc. U. K.* **1983**, *63*, 261−271.

(6) Yule, A. B.; Walker, G. Settlement of *Balanus Balanoides*: The Effect of Cyprid Antennular Secretion. *J. Mar. Biol. Assoc. U.K.* **1985**, *65*, 707−712.

(7) Matsumura, K.; Manami, N.; Yoshinaga, Y. K.; Yamazaki, M.; Clare, A. S.; Fusetani, N. Immunological Studies on the Settlement Inducing Protein Complex (SIPC) of the Barnacle *Balanus Amphitrite* and Its Possible Involvement in Larva-larva Interactions. *Proc. R. Soc. B* **1998**, *260*, 1825−1830.

(8) Dreanno, C.; Matsumura, K.; Dohmae, N.; Takio, K.; Hirota, H.; Kirby, R. R.; Clare, A. S. An α_2-macroglobulin-like Protein Is the Cue to Gregarious Settlement of the Barnacle *Balanus Amphitrite*. *Proc. Natl. Acad. Sci. U.S.A.* **2006**, *103*, 14396−14401.

(9) Dreanno, C.; Kirby, R. R.; Clare, A. S. Smelly Feet Are not Always a Bad Thing: The Relationship Between Cyprid Footprint Protein and the Barnacle Settlement Pheromone. *Biol. Lett.* **2006**, *2*, 423−425.

(10) Callow, J. A.; Callow, M. E. Trends in the Development of Environmentally Friendly Fouling-resistant Marine Coatings. *Nat. Commun.* **2011**, *2*, 244.

(11) Walker, G.; Yule, A. B. Temporary Adhesion of The Barnacle Cyrpids: The Exsitence of an Antennular Adhesive Secretion. *J. Mar. Biol. Assoc. U.K.* **1984**, *64*, 679−686.

(12) Clare, A. S.; Notta, J. A. Scanning Electron Microscopy of the Fourth Antennular Segment of *Balanus Amphitrite Amphitrite*. *J. Mar. Biol. Assoc. U.K.* **1994**, *74*, 967−970.

(13) Andersson, O.; Ekblad, T.; Aldred, N.; Clare, A. S.; Liedberg, B. Novel Application of Imaging Surface Plasmon Resonance for in Situ Studies of the Surface Exploration of Marine Organisms. *Biointerphases* **2009**, *4*, 65−68.

(14) Phang, I. Y.; Aldred, N.; Clare, A. S.; Vancso, G. J. Towards a Nanomechanical Basis for Temporary Adhesion in Barnacle Cyprids (*Semibalanus Balanoides*). *J. R. Soc. Interface.* **2008**, *5*, 397−401.

(15) Guo, S.; Khoo, B. C.; Teo, S. L. M; Zhong, S.; Lim, C. T.; Lee, H. P. Effect of Ultrasound on Cyprid Footprint and Juvenile Barnacle Adhesion on a Fouling Release Material. *Colloids Surf., B* **2014**, *115*, 118−124.

(16) Aldred, N.; Høeg, J. T.; Maruzzo, D.; Clare, A. S. Analysis of the Behaviours Mediating Barnacle Cyprid Reversible Adhesion. *PLoS One* **2013**, *8*, e68085.

(17) Schön, P. M.; Kutnyanszky, E.; Donkelaar, S. F. P.; Santonicola, M.; Tecim, T.; Aldred, N.; Clare, A. S.; Vancso, G. J. Probing Biofouling Resistant Polymer Brush Surfaces by Atomic Force Microscopy Based Force Spectroscopy. *Colloids Surf., B* **2013**, 923−930.

(18) Lee, H.; Scherer, N. F.; Messersmith, P. B. Single-molecule Mechanics of Mussel Adhesion. *Proc. Natl. Acad. Sci. U.S.A.* **2006**, *103*, 12999−13003.

(19) Roach, P.; Farrar, D.; Perry, C. C. Interpretation of Protein Adsorption: Surface-induced Conformational Changes. *J. Am. Chem. Soc.* **2005**, *127*, 8168−8173.

(20) Rabe, M.; Verdes, D.; Seeger, S. Understanding Protein Adsorption Phenomena at Solid Surfaces. *Adv. Colloid Interface Sci.* **2011**, *162*, 87−106.

(21) Sigal, G. B.; Mrksich, M.; Whitesides, G. M. Effect of Surface Wettability on the Adsorption of Proteins and Detergents. *J. Am. Chem. Soc.* **1998**, *120*, 3464−3473.

(22) Arima, Y.; Iwata, H. Effect of Wettability and Surface Functional Groups on Protein Adsorption and Cell Adhesion Using Well-defined Mixed Self-assembled Monolayers. *Biomaterials* **2007**, *28*, 3074−3082.

(23) Faucheux, N.; Schweiss, R.; Lutzow, K.; Werner, C.; Groth, T. Self-assembled Monolayers with Different Terminating Groups as Model Substrates for Cell Adhesion Studies. *Biomaterials* **2004**, *25*, 2721−2730.

(24) Xu, L. C.; Siedlecki, C. A. Effects of Surface Wettability and Contact Time on Protein Adhesion to Biomaterial Surfaces. *Biomaterials* **2007**, *28*, 3273−3283.

(25) Rittschof, D.; Costlow, J. D. Bryozoan and Barnacle Settlement in Relation to Initial Surface Wettability: a Comparison of Laboratory and Field Studies. *Sci. Mar.* **1989**, *53*, 411−416.

(26) Brady, R. F.; Singer, I. L. Mechanical Factors Favoring Release from Fouling Release Coatings. *Biofouling* **2000**, *15*, 73−81.

(27) Qian, P. Y.; Rittschof, D.; Sreedhar, B. Macrofouling in Unidirectional Flow: Miniature Pipes as Experimental Models for Studying the Interaction of Flow and Surface Characteristics on the Attachment of Barnacle, Bryozoan and Polychaete Larvae. *Mar. Ecol.: Prog. Ser.* **2000**, *207*, 109−121.

(28) Hung, O. S.; Thiyagarajan, V.; Qian, P. Y. Preferential Attachment of Barnacle Larvae to Natural Multi-species Biofilms: Does Surface Wettability Matter? *J. Exp. Mar. Biol. Ecol.* **2008**, *361*, 36−41.

(29) Finlay, J. A.; Bennett, S. M.; Brewer, L. H.; Sokolova, A.; Clay, G.; Gunari, N.; Meyer, A. E.; Walker, G. C.; Wendt, D. E.; Callow, M. E.; Callow, J. A.; Detty, M. R. Barnacle Settlement and the Adhesion of Protein and Diatom Microfouling to Xerogel Films with Varying Surface Energy and Water Wettability. *Biofouling* **2010**, *26*, 657−666.

(30) Maki, J. S.; Yule, A. B.; Rittschof, D.; Mitchell, R. The Effect of Bacterial Films on the Temporary Adhesion and Permanent Fixation of Cypris Larvae, *Balanus Amphitrite* Darwin. *Biofouling* **1994**, *8*, 121−131.

(31) Petrone, L.; Di Fino, A.; Aldred, N.; Sukkaew, P.; Ederth, T.; Clare, A. S.; Liedberg, B. Effects of Surface Charge and Gibbs Surface Energy on the Settlement Behaviour of Barnacle Cyprids (*Balanus Amphitrite*). *Biofouling* **2011**, *27*, 1043−1055.

(32) Di Fino, A.; Petrone, L.; Aldred, N.; Ederth, T.; Liedberg, B.; Clare, A. S. Correlation between Surface Chemistry and Settlement Behaviour in Barnacle Cyprids (*Balanus Improvisus*). *Biofouling* **2014**, *30*, 143−152.

(33) Rittschof, D.; Lai, C. H.; Kok, L. M.; Teo, S. L. M. Pharmaceuticals as Antifoulants: Concept and Principles. *Biofouling* **2003**, *19*, 207−212.

(34) Hutter, J. L.; Bechhoefer, J. Calibration of Atomic-force Microscope Tips. *Rev. Sci. Instrum.* **1993**, *64*, 1868−1873.

(35) Riener, C. K.; Stroh, C. M.; Ebner, A.; Klampfl, C.; Gall, A. A.; Romanina, C.; Lyubchenko, Y. L.; Hinterdorfer, P.; Gruber, H. J. Simple Test System for Single Molecule Recognition Force Microscopy. *Anal. Chim. Acta* **2003**, *479*, 59−75.

(36) Barattin, R.; Voyer, N. Chemical Modifications of AFM Tips for the Study of Molecular Recognition Events. *Chem. Commun.* **2008**, 1513−1532.

(37) Yersin, A.; Hirling, H.; Steiner, P.; Magnin, S.; Regazzi, R.; Huni, B.; Huguenot, P.; De Los Rios, P.; Dietler, G.; Catsicas, S.; Kasas, S. Interactions between Synaptic Vesicle Fusion Proteins Explored by Atomic Force Microscopy. *Proc. Natl. Acad. Sci. U.S.A.* **2003**, *100*, 8736−8741.
(38) Patel, A. B.; Allen, S.; Davies, M. C.; Roberts, C. J.; Tendler, S. J. B.; Willams, P. M. Influence of Architecture on the Kinetic Stability of Molecular Assemblies. *J. Am. Chem. Soc.* **2004**, *126*, 1318−1319.
(39) Roduit, C.; van der Goot, F. G.; De Los Rios, P.; Yersin, A.; Steiner, P.; Dietler, G.; Catsicas, S.; Lafont, F.; Kasas, S. Elastic Membrane Heterogeneity of Living Cells Revealed by Stiff Nanoscale Membrane Domains. *Biophys. J.* **2008**, *94*, 1521−1532.
(40) Barattin, R.; Voyer, N. Chemical Modifications of Atomic Force Microscopy Tips. *Methods Mol. Biol.* **2011**, *736*, 457−483.
(41) Pérez-Roa, R. E.; Anderson, M. A.; Rittschof, D.; Orihuel, B.; Wendt, D.; Kowalke, G. L.; Noguera, D. R. Inhibition of Barnacle (*Amphibalanus Amphitrite*) Cyprid Settlement by Means of Localized, Pulsed Electric Fields. *Biofouling* **2008**, *24*, 177−184.
(42) Finlay, J. A.; Callow, M. E.; Ista, L. K.; Lopez, G. P.; Callow, J. A. The Influence of Surface Wettability on the Adhesion Strength of Settled Spores of the Green Alga Enteromorpha and the Diatom Amphora. *Integr. Comp. Biol.* **2002**, *42*, 1116−1122.
(43) Manova, R. K.; Pujari, S. P.; Weijers, C. A. G. M.; Zuilhof, H. Copper-Free Click Biofunctionalization of Silicon Nitride Surfaces via Strain-Promoted Alkyne-Azide Cycloaddition Reactions. *Langmuir* **2012**, *28*, 8651−8663.
(44) Phang, I. Y.; Chaw, K. C.; Choo, S. S. H.; Kang, R. K. C.; Lee, S. S. C; Birch, W. R.; Teo, S. L. M; Vancso, G. J. Marine Biofouling Field Tests, Settlement Assay and Footprint Micromorphology of Cyprid Larvae of *Balanus Amphitrite* on Model surfaces. *Biofouling* **2009**, *25*, 139−147.
(45) Sethuraman, A.; Han, M.; Kane, R. S.; Belfort, G. Effect of Surface Wettability on the Adhesion of Proteins. *Langmuir* **2004**, *20*, 7779−7788.
(46) Wertz, C. F.; Santore, M. M. Effect of Surface Hydrophobicity on Adsorption and Relaxation Kinetics of Albumin and Fibrinogen: Single-species and Competitive Behavior. *Langmuir* **2001**, *17*, 3006−3016.
(47) Agnihotri, A.; Soman, P.; Siedlecki, C. A. AFM Measurements of Interactions between the Platelet Integrin Receptor GPIIbIIIa and Fibrinogen. *Colloids Surf., B* **2009**, *71*, 138−147.
(48) Fantner, G. E.; Hassenkam, T.; Kindt, J. H.; Weaver, J. C.; Birkedal, H.; Pechenik, L.; Cutroni, J. A.; Cidade, G. A.; Stucky, G. D.; Morse, D. E.; Hansma, P. K. Sacrificial Bonds and Hidden Length Dissipate Energy as Mineralized Fibrils Separate during Bone Fracture. *Nat. Mater.* **2005**, *4*, 612−616.
(49) Phang, I. Y.; Aldred, N.; Ling, X. Y.; Huskens, J.; Clare, A. S.; Vancso, G. J. Atomic Force Microscopy of the Morphology and Mechanical Behaviour of Barnacle Cyprid Footprint Proteins at the Nanoscale. *J. R. Soc. Interface.* **2010**, *7*, 285−296.
(50) Phang, I. Y.; Aldred, N.; Ling, X. Y.; Tomczak, N.; Huskens, J.; Clare, A. S.; Vancso, G. J. Chemistry-specific Interfacial Forces between Barnacle (*Semibalanus Balanoides*) Cyprid Footprint Proteins and Chemically Functionalised AFM tips. *J. Adhes.* **2009**, *85*, 616−630.
(51) Park, B. J.; Abu-Lail, N. I. Atomic Force Microscopy Investigations of Heterogeneities in the Adhesion Energies Measured between Pathogenic and Non-pathogenic Listeria Species and Silicon Nitride as They Correlate to Virulence and Adherence. *Biofouling* **2011**, *27*, 543−549.
(52) Lee, J. H.; Lee, H. B. Platelet Adhesion onto Wettability Gradient Surfaces in the Absence and Presence of Plasma Proteins. *J. Biomed. Mater. Res.* **1998**, *41*, 304−311.
(53) Yu, J.; Kan, Y.; Rapp, M.; Danner, E.; Wei, W.; Das, S.; Miller, D. R.; Chen, Y.; Waite, J. H.; Israelachvili, J. N. Adaptive Hydrophobic and Hydrophilic Interactions of Mussel Foot Proteins with Organic Thin Films. *Proc. Natl. Acad. Sci. U.S.A.* **2013**, *110*, 15680−15685.
(54) Palacio, M. L.; Schricker, S. R.; Bhushan, B. Bioadhesion of Various Proteins on Random, Diblock and Triblock Copolymer Surfaces and the Effect of pH Conditions. *J. R. Soc. Interface.* **2011**, *8*, 630−640.
(55) Merkel, R.; Nassoy, P.; Leung, A.; Ritchie, K.; Evans, E. Energy Landscapes of Receptor-ligand Bonds Explored with Dynamic Force Spectroscopy. *Nature* **1999**, *397*, 50−53.
(56) Zou, S.; Schönherr, H.; Vancso, G. J. Force Spectroscopy of Quadruple H-bonded Dimers by AFM: Dynamic Bond Rupture and Molecular Time-temperature Superposition. *J. Am. Chem. Soc.* **2005**, *127*, 11230−12231.
(57) Mondon, M.; Berger, S.; Ziegler, C. Scanning-force Techniques to Monitor Time-dependent Changes in Topography and Adhesion Force of Proteins on Surfaces. *Anal. Bioanal. Chem.* **2003**, *375*, 849−55.
(58) Quintana, R.; Gosa, M.; Jańczewski, D.; Kutnyanszky, E.; Vancso, G. J. Enhanced Stability of Low Fouling Zwitterionic Polymer Brushes in Seawater with Diblock Architecture. *Langmuir* **2013**, *29*, 10859−10867.
(59) Aldred, N.; Li, G.; Gao, Y.; Clare, A. S.; Jiang, S. Modulation of Barnacle (*Balanus Amphitrite* Darwin) Cyprid Settlement Behavior by Sulfobetaine and Carboxybetaine Methacrylate Polymer Coatings. *Biofouling* **2010**, *26*, 673−683.
(60) Quintana, R.; Jańczewski, D.; Vasantha, V. A.; Jana, S.; Lee, S. S. C.; Parra Velandia, F. J.; Guo, S.; Parthiban, A.; Teo, S. L. M.; Vancso, G. J. Sulfobetaine-based Polymer Brushes in Marine Environment: Is There an Effect of the Polymerizable Group on the Antifouling Performance? *Colloids Surf.,B* **2014**, *120*, 118−124.